J Appl Physiol 102: 1329–1340, 2007.
First published December 14, 2006; doi:10.1152/japplphysiol.00805.2006.

A theoretical model of selective cooling using intracarotid cold saline infusion in the human brain

Angelos-Aristeidis Konstas,[1]* Matthew A. Neimark,[2]* Andrew F. Laine,[1,2] and John Pile-Spellman[1]
Departments of [1]Radiology and [2]Biomedical Engineering, Columbia University, New York, New York

Submitted 20 July 2006; accepted in final form 12 December 2006

Konstas AA, Neimark MA, Laine AF, Pile-Spellman J. A theoretical model of selective cooling using intracarotid cold saline infusion in the human brain. *J Appl Physiol* 102: 1329–1340, 2007. First published December 14, 2006; doi:10.1152/japplphysiol.00805.2006.—A three-dimensional mathematical model was developed to examine the transient and steady-state temperature distribution in the human brain during selective brain cooling (SBC) by unilateral intracarotid freezing-cold saline infusion. To determine the combined effect of hemodilution and hypothermia from the cold saline infusion, data from studies investigating the effect of these two parameters on cerebral blood flow (CBF) were pooled, and an analytic expression describing the combined effect of the two factors was derived. The Pennes bioheat equation used the thermal properties of the different cranial layers and the effect of cold saline infusion on CBF to propagate the evolution of brain temperature. A healthy brain and a brain with stroke (ischemic core and penumbra) were modeled. CBF and metabolic rate data were reduced to simulate the core and penumbra. Simulations using different saline flow rates were performed. The results suggested that a flow rate of 30 ml/min is sufficient to induce moderate hypothermia within 10 min in the ipsilateral hemisphere. The brain with stroke cooled to lower temperatures than the healthy brain, mainly because the stroke limited the total intracarotid blood flow. Gray matter cooled twice as fast as white matter. The continuously falling hematocrit was the main time-limiting factor, restricting the SBC to a maximum of 3 h. The study demonstrated that SBC by intracarotid saline infusion is feasible in humans and may be the fastest method of hypothermia induction.

therapeutic hypothermia; ischemic stroke; spatial and temporal brain temperature distributions

THE CENTRAL NERVOUS SYSTEM is vulnerable to focal and global ischemia resulting from acute ischemic stroke (63) and cardiac arrest (21). Therapeutic hypothermia has been repeatedly shown to be effective in limiting the damage of global and focal ischemia in animal models and clinical studies (6, 21).

In most clinical studies, hypothermia is induced by surface cooling. Although this is the simplest and most cost-effective option for inducing hypothermia (14), it has two major drawbacks. *1*) Several hours are required to reach the target body core temperature. All studies report a 3- to 7-h period for cooling to 32–34°C (26, 52); however, endovascular systemic cooling may be able to accelerate the rate of cooling and improve the efficacy of hypothermia (15). *2*) The incidence of adverse effects, such as impaired immune function, decreased cardiac output, pneumonia, and cardiac arrhythmias/bradycardias, is high (14, 31). Selective brain cooling (SBC) without reducing body core temperature can theoretically address both problems of whole body cooling.

Different methods for SBC have been reported (18). Noninvasive methods most commonly used are cooling caps and helmets. However, theoretical analyses (11, 44, 60) and empirical measurements (8, 35) suggest that such measures are effective in reducing the temperature in the superficial cerebral regions, but not in deep brain structures.

One potential method of SBC is intracarotid cold saline infusion (ICSI). Cold saline is infused into the internal carotid artery (ICA) via transfemoral catheterization. This method would potentially be much faster than whole body cooling and more effective than surface SBC.

The aim of the present study is to address three issues that determine the potential clinical feasibility of ICSI. *1*) What minimum brain temperatures can be achieved by different rates of ICSI? *2*) How rapidly can the ICSI cool the brain? *3*) How will different infusion rates affect hematocrit, and will hemodilution limit the length of the procedure?

THEORY AND METHODS

In the first part of the present study, data were pooled from studies investigating the effect of hypothermia and hemodilution on CBF to derive an analytic expression of the combined effect of these two parameters on CBF during ICSI. In the second part, a hemispherical three-dimensional theoretical model was developed to examine the transient and steady-state temperature response to SBC with different flow rates of cold saline in the ICA. The effect of regionally reduced blood perfusion rates in the brain tissue during focal ischemia is also examined. The time to reach the target hypothermic temperature is estimated corresponding to different cold saline infusion rates in healthy and ischemic adult brain models. (See the *Glossary* in the online version of this article for the symbols used in this study.)

Criteria for inclusion of experimental studies in the present analysis. A PubMed search was performed for all studies that investigated *1*) the effect of temperature on cerebral blood flow (CBF), *2*) the effect of hematocrit on CBF, and *3*) the effect of hemodilution on hematocrit. For studies of the effect of temperature on CBF, human and animal studies addressing the effect of temperature on CBF were pooled. For the effect of hematocrit on CBF, only human studies were included. Healthy subjects and subjects with various cerebral conditions were included. For the effect of hemodilution on hematocrit, only human studies of hypervolemic hemodilution using normal saline were included.

Effect of temperature and hematocrit on CBF. Michenfelder and Milde (39) demonstrated that lowering brain temperatures from 37 to 27°C decreased the metabolic rate by a factor of 3 ($Q_{10} = 3$). Thus

* A.-A. Konstas and M. A. Neimark contributed equally to this work.

Address for reprint requests and other correspondence: M. A. Neimark, Dept. of Biomedical Engineering, Columbia Univ., New York, New York 10027 (e-mail: man2003@columbia.edu).

The costs of publication of this article were defrayed in part by the payment of page charges. The article must therefore be hereby marked "*advertisement*" in accordance with 18 U.S.C. Section 1734 solely to indicate this fact.

metabolic heat production of the brain was formulated by Xu et al. (68) as follows

$$q = q_0 \cdot 3^{\frac{T-37}{10}} \quad (1)$$

where q_0 is the baseline metabolic rate at 37°C and T is temperature. Animal studies suggest that, during circulatory arrest, the reduction of metabolic rate nearly parallels the decrease in CBF (22). Moreover, there is direct evidence of coupling of CBF to cerebral oxygen metabolism from swine (12, 62) and dog (39) studies. However, there is also evidence of uncoupling between CBF and cerebral oxygen metabolism during deep (20–26°C) and profound (<20°C) cooling (12, 39).

Given the data in the literature relating CBF to temperature, a more precise formulation of the exponential relation between these two quantities could be determined. It was assumed that CBF was coupled to cerebral metabolic rate with brain temperatures as low as 25°C; thus the temperature-dependent CBF could be expressed as

$$\omega = \omega_0 \cdot \alpha^{\beta(T-37)} \quad (2)$$

where ω_0 is baseline perfusion. Similarly, the relation between brain metabolism and temperature could be expressed as

$$q = q_0 \cdot \alpha^{\beta(T-37)} \quad (3)$$

Data points from the studies listed in Table 1 were fit by *Eq. 2*. The root-mean-square error (RMSE) between the data points and *Eq. 2* was minimized by varying α and β through the unconstrained nonlinear optimization (*fminunc* function in Matlab). The RMSE was derived by subtracting the equation point values from the recorded data for corresponding temperatures, squaring the difference, summing, and dividing the result by the degrees of freedom (number of data points reduced by 2 because of the 2 data points that are needed to estimate the 2 parameters). Data for CBF changes at <25°C were not used in this analysis for two reasons: *1*) temperatures <25°C are not likely to be used in therapeutic hypothermia, and *2*) there is evidence of uncoupling between CBF and cerebral oxygen metabolism at deep (20–26°C) and profound (<20°C) hypothermia, suggesting that autoregulation of CBF in accordance with metabolic needs is not preserved (12, 39).

There is a nearly linear relation between mild and moderate hemodilution (Hct >30) and CBF (34). Data points from the studies listed in Table 2 were fit by the following linear function

$$\omega = \omega_0 \cdot (1 - \gamma\Delta_{Hct}) \quad (4)$$

The mean RMSE between the data points and *Eq. 4* was minimized by linear least squares fitting. In this case, the number of degrees of freedom was reduced by 1 to calculate RMSE.

A linear relation similar to that of hematocrit and CBF at 37°C was assumed for all other temperatures (i.e., utilizing the same value of γ). The combined effect of temperature and hematocrit on CBF was expressed as

$$\omega_c = \omega_0 \cdot \alpha^{\beta(T-37)}(1 - \gamma\Delta_{Hct}) \quad (5)$$

where ω_c is the temperature- and hematocrit-corrected perfusion.

Effect of infusion volume on hematocrit. When the bloodstream is infused with isotonic saline, part of it enters the extravascular space. The remaining volume of saline hemodilutes the blood. An expression for the resulting change of hematocrit is

$$\Delta_{Hct} = \frac{-pV_{RBC}\,\Delta V_{IV}}{V_{IV(0)}\,[V_{IV(0)} + p\Delta V_{IV}]} \quad (6)$$

where V_{RBC} is the total red blood cell volume, $V_{IV(0)}$ is the initial total intravascular volume (including V_{RBC}), ΔV_{IV} is the volume of added saline, and p is the fraction of extracellular water that is intravascular.

Table 1. *Animal and human studies of CBF-temperature relation*

Ref.	Disease/Condition	Cooling Method	Target Temp, °C	CBF Change, %	CBF Change/1°C, %
		Pigs			
Ehrlich et al. (12)	Healthy	CPB	(37), 28, 18	−48, −64	−5.3
Bauer et al. (3)	Increased ICP	External systemic	(38), 32	−26	−4.3
Walter et al. (62)	Healthy	Intracerebral with extracorporeal cooling	(38), 30, 25	−40, −61	−5
		Dogs			
Rosomoff & Holaday (48)	Healthy	External systemic	(35), 30, 26	−35, −63	−7
Michenfelder & Milde (39)	Healthy	CPB	(37), 27, 22, 18, 14	−46, −59, −42, −58	−4.6
Michenfelder et al. (40)	Global cerebral ischemia	External systemic and extracorporeal	(37), 40	+20	+6.7
		Cats			
Mori et al. (41)	Healthy	External systemic	(37), 33, 29	−56, −77	−14
		Baboons			
Schwartz et al. (53)	Healthy	Intracerebral with extracorporeal cooling	(37), 24.5	−59	−4.7
		Humans			
Marion et al. (33)	Severe head injury	External systemic and gastric lavage	(37), 33	−26	−6.5
Shiozaki et al. (55)	Severe head injury	External systemic	(37), 34	−50	−16.7
Metz et al. (38)	Severe head injury	External systemic	(37), 33	0	0
Kawamura et al. (28)	SAH	External systemic	(37), 34	−37	−12.3
Jalan et al. (23)	ALF-induced intracranial hypertension	External systemic	(37), 32.5	−57	−12.7
Jalan et al. (24)	OLT-induced hyperemia in ALF patients	External systemic	(37), 33	−32	−8

ICP, intracranial pressure; CPB, cardiopulmonary bypass; SAH, sabarachnoid aneurysm; ALF, acute liver failure; OLT, orthotopic liver transplantation; CBF, cerebral blood flow. Values in parentheses are initial temperatures for each study. CBF change/1°C is calculated from the first CBF change in studies where >1 step of hypothermia was performed.

Table 2. *Human studies of CBF-hematocrit relation*

Ref.	Disease/Condition	Hemodilution Method	Hct Change, %	CBF Change, %	CBF Change/HCT, %
Henriksen et al. (19)	Healthy with high Hct	Normovolemic	−9, −13	+19, +23	+2.1
Hino et al. (20)	Healthy volunteers	Normovolemic	−5	+6	+1.2
Vorstrup et al. (61)	Acute ischemic stroke	Normovolemic	−7	+21	+3
Origitano et al. (46)	SAH	"Triple-H"	−9	+21	+2.3
Wood et al. (65)	Stroke patients with temporal-MCA bypass	Normovolemic	−7	+23	+3.3
Ekelund et al. (13)	SAH	Normovolemic	−8	+12	+1.5
Tu & Liu (59)	Healthy volunteers	Normovolemic	−12	+35	+2.9
Muhling et al. (42)	Healthy volunteers	Normovolemic	−12	+26*	+2.2*
Bruder et al. (5)	Anesthetized patients with aneurism of tumor	Normovolemic	−8	+16*	+2*

"Triple-H", hypertension, hypervolemia, and hemodilution; MCA, middle cerebral artery. *CBF velocities were used.

An initial hematocrit of 42% and a $V_{IV(0)}$ of 5.0 liters is assumed (implying $V_{RBC} = 2.1$ liters).

In the steady state, p is normally 0.25–0.33 (1). However, since therapy will take place over relatively short periods of time relative to the time for intravascular volume to reach equilibrium, p should be somewhat higher in practice. To determine a working value of p, *Eq. 6* was fit with the data in Table 3 by unconstrained nonlinear optimization. The number of degrees of freedom was reduced by 1 for calculation of RMSE.

Heat exchange between an insulated catheter and blood. From the femoral artery to the arch of the aorta, there is a counterflow between cold saline in the catheter and the blood. From the aortic arch and in the carotid artery, the coolant flows parallel to the blood. Heating of the cold saline flowing in the catheter is an important factor that determines the feasibility of ipsilateral intracerebral cooling. Hence, an experiment was conducted to determine the temperature increase of freezing-cold saline between injection at the femoral artery and the carotid artery bifurcation at different flow rates. A life-sized phantom model of the human arterial tree extending from the common femoral bifurcation to the ICAs (Flowtek) was used. Warm water was pumped continuously through the model, inflow via the ascending aorta and outflow via the common iliac artery and left ICA, to closely reproduce the blood flow in the human arterial tree.

To create a thermally insulated catheter, a 100-cm 5-F catheter (Torcon NB Advantage, Cook, Bloomington, IN) was inserted into a 90-cm 8-F guiding catheter (Cordis, Miami, FL), with the distal tip of the 5-F catheter extending 2 cm distally from the distal tip of the guiding catheter. The two catheters were glued together at the tip of the guiding catheter, resulting in an air-filled guiding catheter (since air is an excellent thermal insulator). The inlet temperature of the saline was lowered to subzero temperatures by addition of salt to the ice bath surrounding the saline bag. The insulated catheter was introduced to the model through the right femoral bifurcation, and the distal tip was navigated to the left common carotid artery bifurcation. Outlet temperature was monitored with a fluoroptic temperature probe (Luxtron, Santa Clara, CA) that was inserted into the 5-F catheter and reached within 1 cm from the tip of the catheter. A second probe monitored the inlet temperature, and a third probe was inserted via the right ICA to monitor the temperature of the warm water in the model. The outlet temperature was recorded for different saline flow rates. The resulting predicted temperature of the mixture of cold saline with blood (e.g., cold perfusate) was calculated as follows

$$T_{cp} = \frac{\text{ICA blood flow} \cdot 37^{\circ}\text{C} + \text{saline flow} \cdot T_o}{\text{ICA blood flow} + \text{saline flow}} \quad (7)$$

where T_{cp} is the temperature of the cold perfusate and T_o is the outlet temperature. ICA blood flow was assumed to be 250 ml/min (4, 45, 50, 51).

Theoretical model of SBC using ICSI. The geometry modeled was a hemisphere of cerebral tissue with overlying layers of skull and scalp (11) (Fig. 1, *A* and *B*). Appropriate physical and physiological characteristics were assigned to each component on the basis of values obtained from the literature (Table 4). The scalp was assigned a thickness of 4 mm and thermal and perfusion characteristics that represent a blend of muscle, fat, fascia, and skin. The skull was assigned a thickness of 4 mm, low conductivity, and perfusion rate and metabolic rate typical of cancellous bone. The anatomic brain model had an 85-mm radius, yielding a volume of 1,285 ml, a value between that of the average human male and that of the average female brain (29). The anterior circulation (ICA) carries 75% of the brain's blood supply and comprises 75% of the total vascular volume, while the posterior circulation (vertebrals) supplies the remaining 25%. These values accurately reflect the relative contributions of the anterior and posterior circulation, derived through color duplex sonography and phase-contrast MRI, that range from 67% to 82% for the ICAs (4, 45, 50, 51). Given that the ipsilateral ICA perfused three-quarters of the corresponding brain hemisphere, the brain volume receiving the intra-arterial cold perfusate was 482 ml, and the corresponding brain mass was 496 g. The model assumed no mixing of blood between the posterior and anterior circulations and a sharp demarcation of the two vascular sections without arterial boundary zones (Fig. 1). The model differentiated between white and gray matter, because they have similar thermal properties but different

Table 3. *Effect of hypervolemic hemodilution with normal saline on hematocrit*

Ref.	Disease/Condition	Infusion Volume, ml	Infusion Time, min	Infusion Rate, ml/min	Hct Change, %
Stamler (57)	Healthy volunteers and renal colic	1,400	45	31.1	−4.8
Grathwohl et al. (16)	Healthy volunteers	2,277	30	75.9	−4.1
Wysocki et al. (66)	Hypertensive patients	1,000	12.5	80	−4.7
Wysocki et al. (67)	Hypertensive patients	1,000	13.5	74.1	−3.4
Johansen et al. (25)	Healthy volunteers	1,500	21	71.4	−4
Kass et al. (27)	Healthy volunteers	1,050	30	35	−4.5
Greenfield et al. (17)	Healthy volunteers	715	6–7	115	−4.5
Greenfield et al. (17)	Healthy volunteers	1,481	13	115	−6.1
Greenfield et al. (17)	Healthy volunteers	2,242	19.5	115	−6.3

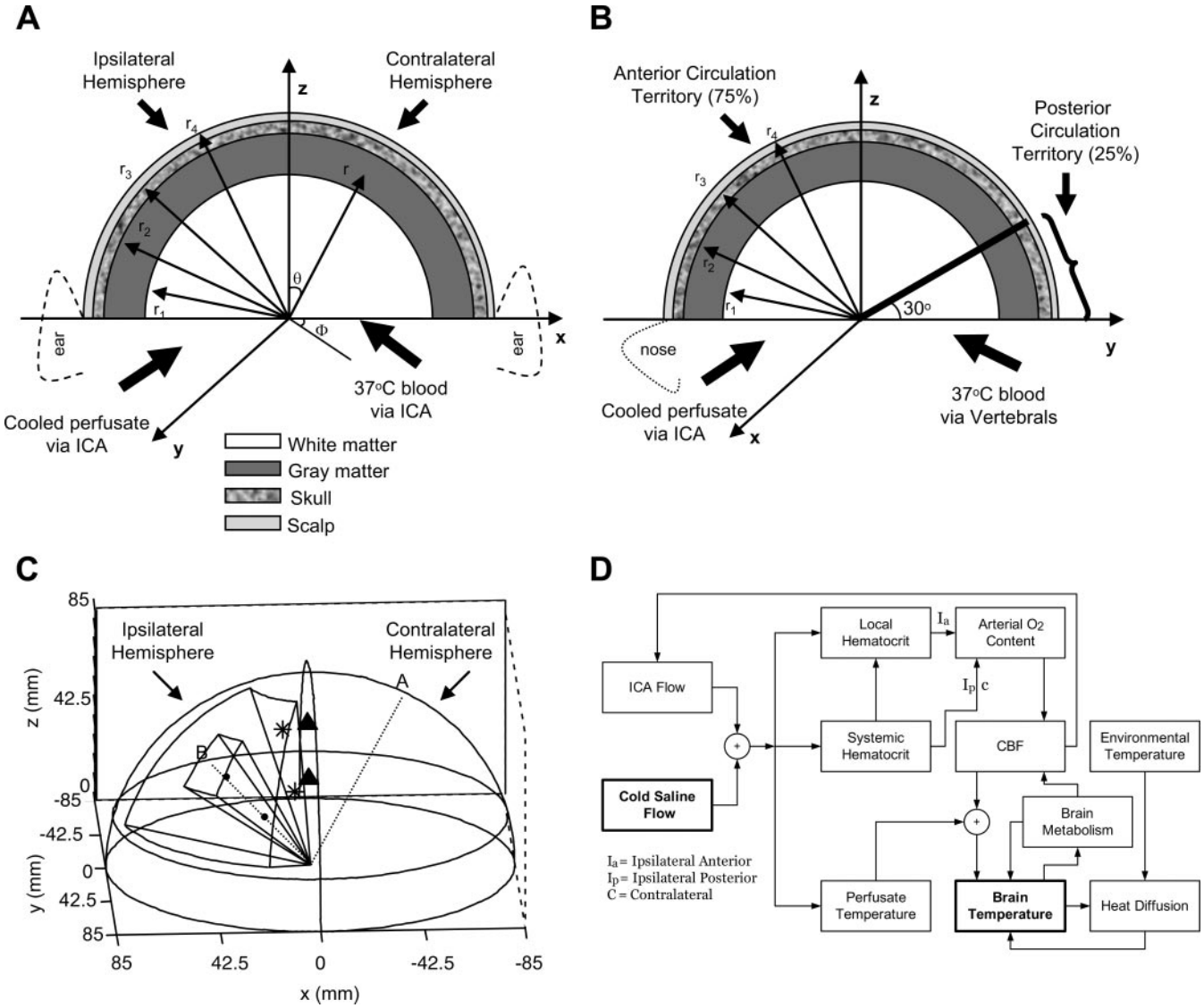

Fig. 1. Anatomic structure of the head model. The brain is modeled as a hemisphere. *A*: coronal section of the model. *B*: paramedian section of the model. *C*: 3-dimensional representation of the brain, with the ischemic core and an outer penumbra simulated as spherical sections (not to scale). Various tissue layers are omitted for simplicity. V-shaped *A-B* line starts at a latitude of 45°, descends to the center-base of the brain, and ascends back to the same latitude, in a longitudinal plane from −135° to +45°. Longitudinal plane dissects the posterior circulation territory of the contralateral hemisphere to the anterior territory of the ipsilateral hemisphere via the center of the brain. Radial temperature distribution in Fig. 3 is along line *A-B*. ●, Temperature-sampling points in Fig. 5, *A* and *B* (and also in Fig. 4; but without the stroke); ∗, temperature-sampling points in Fig. 5, *C* and *D*; ▲, temperature-sampling points in Fig. 5, *E* and *F*. *D*: flow chart of the brain model.

metabolic and perfusion rates (Table 4). The perfusion of the gray and white matter was 80 and 20 ml·min^{-1}·100 g^{-1}, respectively, resulting in a mean brain perfusion rate of 50.6 ml·min^{-1}·100 g^{-1}. The total perfusion for the ipsilateral anterior circulation was 256 ml/min, which was in strikingly good agreement with the assumed intracarotid blood flow rate used in the phantom model experiment.

Calculations of heat transfer were based on the accepted bioheat model proposed by Pennes (47), which is represented by the following equation

Table 4. *Physical and physiological properties in the model*

Anatomic Structure	*c,* J·kg^{-1}·K^{-1}	ρ, kg/m^3	*k,* W·m^{-1}·K^{-1}	ω_0, ml·min^{-1}·100 g^{-1}	q_0, W/m^3	r, mm
Blood*	3,800	1,050	0.5	N/A	N/A	N/A
Scalp	4,000	1,000	0.342	2.0	363.4	93
Bone	2,300	1,520	1.16	1.8	368.3	89
Gray matter	3,700	1,030	0.49	80	16,700	85
White matter	3,700	1,030	0.49	20	4,175	67

Values are from Refs. 11, 44, 60, and 68. *c,* specific heat; ρ, mass density; *k,* thermal conductivity; ω_0, perfusion rate; q_0, metabolic rate; *r,* radius. N/A, nonapplicable. *Saline was assumed to have the same physical properties as blood.

$$\frac{\partial T(\vec{x}, t)}{\partial t} = \frac{\nabla \cdot [k(\vec{x}) \nabla T(\vec{x}, t)]}{\rho(\vec{x}) c(\vec{x})} + \frac{\rho_{blood} c_{blood}}{\rho(\vec{x}) c(\vec{x})} \omega_c(\vec{x}, t)[T_{artery}(\vec{x}, t) - T(\vec{x}, t)] + \frac{q(\vec{x}, t)}{\rho(\vec{x}) c(\vec{x})} \quad (8)$$

where T is temperature, k is tissue thermal conductivity, ρ is density, c is heat capacity, ω_c is hematocrit- and temperature-corrected blood perfusion, q is tissue metabolism (also corrected in the brain for temperature), t is time, and $\vec{x}$ is spatial location. The subscript "blood" signifies blood density and heat capacity; the subscript "artery" signifies arterial temperature (37°C without cold saline infusion). Tissue variables and parameters lack a subscript. For brain, *Eqs. 3* and *5* were used to correct ω and q by hematocrit and temperature.

Equation 8 implies that the rate of temperature change in tissue depends on three factors: *1*) heat diffusion, *2*) arterial perfusion, and *3*) metabolism. This is a continuum model and assumes thermal equilibration between capillary blood and the surrounding tissues. Convective heat transfer between the layers was assumed to be negligible, and heat exchange between the layers was attributed to conduction only. This is appropriate, because the larger cerebral arteries are generally directed in an outward radial direction, with the smaller vessels branching in the circumferential direction (44). The principal sites of blood-tissue heat exchange are small arterioles and capillaries; hence, the circulatory heat transfer in the radial direction is minimal. Heat transfer between the brain tissues of the anterior and posterior circulation and between the right and left hemisphere was attributed to conduction only.

Blood perfusion and metabolic rate of ischemic and healthy brain tissue are very different (54). During ischemia, blood perfusion and metabolic rate in the ischemic core were reduced to 25% and 30% of their normal values, respectively. Blood perfusion and metabolic rate were reduced to 40% and 50%, respectively, in the evolving infarct (ischemic penumbra). These reductions in metabolic rate and perfusion are close to those reported in the literature (54) and are given by

$$\omega = \min(\omega_c, 0.25\omega_0), \text{ (ischemic core) and } \omega = \min(\omega_c, 0.4\omega_0) \text{ (ischemic penumbra)} \quad (9)$$

$$q = \min(q_c, 0.3q_0), \text{ (ischemic core) and } q = \min(q_c, 0.5q_0) \text{ (ischemic penumbra)} \quad (10)$$

where ω_0 and q_0 are the blood perfusion and metabolic rates, respectively, under normal conditions (37°C) and ω_c and q_c are temperature- and hematocrit-adjusted parameters from *Eqs. 2* and *5*.

The ischemic stroke was modeled in the right (ipsilateral) frontal quadrant with the following angle demarcations: $\theta = 16$–$54°$ and $\phi = 37.5$–$52.5°$ for stroke core and $\theta = 18$–$36°$ and 54–$72°$ and $\phi = 15$–$37.5°$ and 52.5–$75°$ for ischemic penumbra. The total stroke volume was 136.42 ml, and the volume of the core was 11.87 ml (Fig. 1*C*).

For the territory of the brain perfused by the right ICA, it was necessary to modify the values of hematocrit (which affects perfusion) and T_{artery} in *Eq. 8* because of the cold saline infusion. T_{artery} is determined from *Eq. 7*. Similarly, an expression for the hematocrit dilution effect of the infusion is given by

$$Hct_{local} = \frac{\text{ICA blood flow} \cdot Hct}{\text{ICA blood flow} + \text{saline flow}} \quad (11)$$

ICA blood flow can be calculated by

$$\text{ICA blood flow} = \iiint_{\text{ICA territory}} \omega_c dV \quad (12)$$

where ω_c is the temperature- and hematocrit-dependent brain blood perfusion from *Eq. 5*. However, since additional perfusate volume enters the brain in the ICA territory because of the ICA infusion, ω must be modified as follows for use in *Eq. 8*

$$\omega_{ICA}(r, \theta, \phi) = \omega_c(r, \theta, \phi) + \omega_c(r, \theta, \phi) \frac{\text{saline flow}}{\text{ICA blood flow}} \quad (13)$$

Figure 1*D* summarizes the relations between different physical and physiological components of the model (for more technical details concerning the model's formulation and boundary conditions see the APPENDIX in the online version of this article).

Effect of ICSI on systemic temperature: estimation of maximum theoretical systemic cooling. Average whole body temperature after saline infusion can be determined as follows

$$\frac{dT}{dt} = \frac{dm_i}{dt} \frac{(h_i - h_e)}{m_{body} c} \quad (14)$$

where h is specific enthalpy, c is the average heat capacity (0.83 $kcal \cdot kg^{-1} \cdot K^{-1}$), and m is the mass of infused saline (37). The subscripts "i" and "e" represent inlet and exit, respectively. *Equation 14* is based on the first law of thermodynamics and assumes that *1*) the rate of heat transfer loss and the average rate of heat generation inside the body are equal (~80–100 J/s), *2*) there is no work being performed, and *3*) the patient weighs 70 kg and is able to excrete water and cold saline infusion at the same rate.

All data analysis and numerical simulations were performed in Matlab (Natick, MA).

RESULTS

The animal and human studies that investigated the relation between CBF and temperature are listed in Table 1. Cooling methods used for each study included external systemic cardiopulmonary bypass and/or intracerebral, as well as extracorporeal, cooling. No study used saline infusion or other hemodiluting methods; hence, the CBF change can be attributed solely to the systemic temperature changes that are assumed to reflect corresponding brain temperature changes. The CBF change per 1°C change was very similar in the animal and human studies. Therefore, human and animal data in Table 1 were used to construct Fig. 2*A*, which shows the mean reduction of CBF with temperature drop. Exponential fitting of these data according to *Eq. 3* resulted in $\alpha = 2.961$ and $\beta = 0.08401$ (RMSE = 18.8%), which are similar to values cited previously (11, 39, 68).

Human studies that investigated the relation between CBF and decline in hematocrit (hemodilution) are listed in Table 2. In the two studies that recorded the systemic temperature of the subjects before, during, and after hemodilution, no temperature changes were reported during the procedure (5, 42). In the other seven studies, temperature data were not reported (13, 19, 20, 46, 59, 61, 65); it was thus assumed that the CBF change can be attributed solely to hematocrit changes. Linear fitting of *Eq. 4* resulted in $\gamma = 2.245$ (RMSE = 5.31%); i.e., CBF increased by 2.2%, on average, for each point of hematocrit reduction. Figure 2*B* illustrates the linear relation between decline in hematocrit and increase in CBF.

Fitting *Eq. 6* with the data in Table 3 yielded $p = 0.4217$ (RMSE = 0.0149). This implies that, over short infusion periods, 42% of injected saline remains in the intravascular space. This is a higher value than the expected equilibrium proportion.

ICSI will decrease the hematocrit and the intracerebral temperature simultaneously. Figure 2*C* shows the combined effect of hematocrit and temperature reduction on CBF. A 10%

decline in hematocrit increases CBF by 23%, whereas a 5°C temperature drop reduces CBF by 37%. Hence, the model suggests that hypothermia is the dominant regulatory parameter of CBF, over the physiologically relevant ranges of hematocrit and temperature, during ICSI.

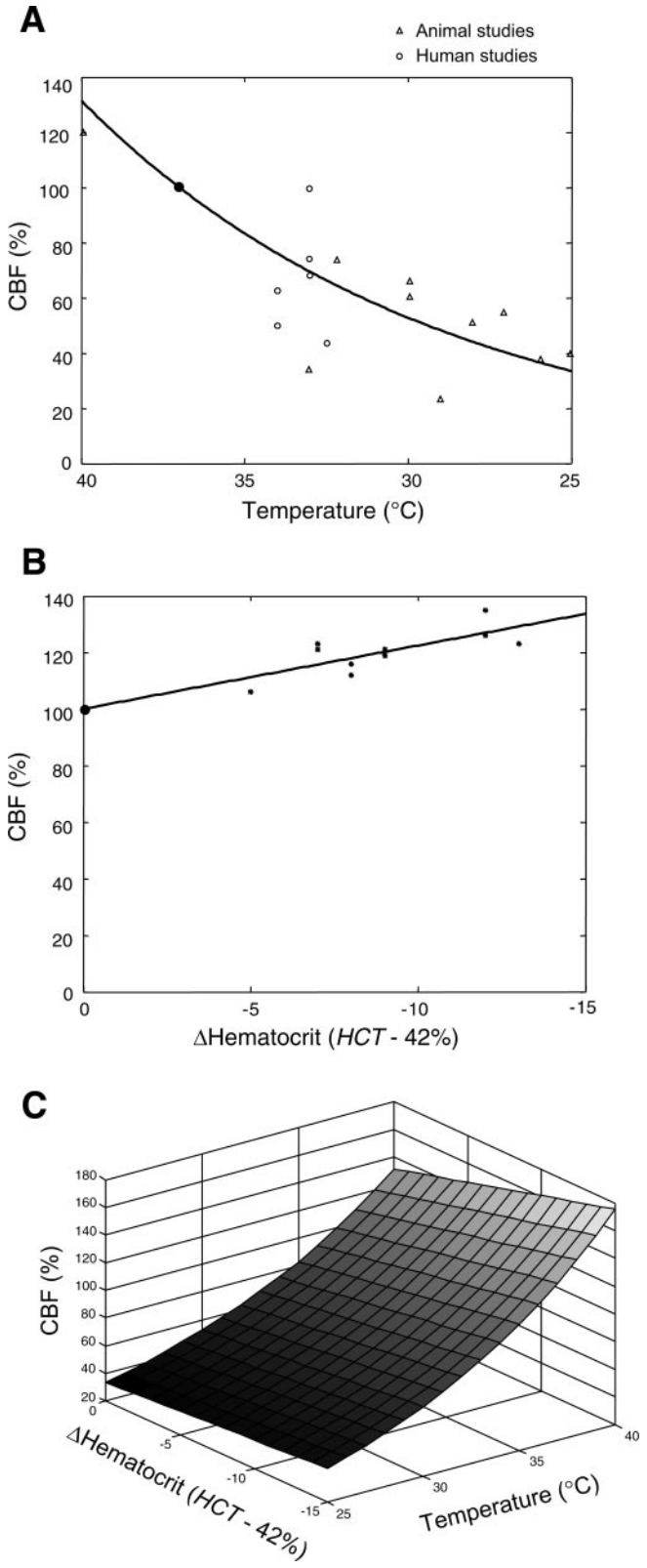

Fig. 2. Effect of temperature and hematocrit on cerebral blood flow (CBF). *A*: CBF decreases with decline of brain temperature. All data points are from studies listed in Table 1. ●, Baseline perfusion at 37°C and 42% Hct. Line represents best fit to data by unconstrained nonlinear optimization [root-mean-square error (RMSE) = 18.36%]. *B*: CBF increases with hemodilution. All data points are from studies listed in Table 2. Line represents best fit to data by linear regression (RMSE = 5.31%). *C*: 3-dimensional surface representing combined effect of temperature and hemodilution on CBF according to *Eq. 5*.

Table 5. *Experimental inlet and outlet temperatures of an insulated catheter and estimation of corresponding cold perfusate temperature*

Saline Flow Rate, ml/min	Inlet Temp, °C	Outlet Temp, °C	Arterial Tree Temp, °C	Initial Cold Perfusate Temp in Healthy Brain/Brain With Stroke, °C
50	−1.2	1.8	37.4	31.8/30.8
40	−1.3	2.5	37.0	32.7/31.7
30	−1.6	2.8	37.4	33.7/32.7
20	−1.7	5.0	36.4	34.8/34.2
10	−1.9	12.1	36.6	36.1/35.8

Table 5 summarizes the temperature of the cold saline at the outlet of the insulated catheter for different flow rates of the saline. These data were used to estimate the temperature of the cold perfusate flowing in the ICA (i.e., blood and cold saline). Higher flow rates resulted in lower temperatures of cold infusate because of the inverse relation of total heat transfer to flow rate. The decrease in heat transfer with increasing flow rate has been reported elsewhere (43).

Figure 3 shows the radial temperature distribution 60 min after different rates of saline infusion along the V-shaped *A-B* line, which starts at a latitude of 45°, descends to the center-base of the brain, and ascends back to the same latitude, in a longitudinal plane from $\phi = -135°$ to $+45°$. This longitudinal plane dissects the posterior circulation territory of the contralateral hemisphere to the anterior territory of the ipsilateral hemisphere via the center of the brain (Fig. 1*C*). Under steady-state conditions (no saline infusion), the white matter temperature was 37.3°C and was homogeneous. This represents deep brain temperature 0.3°C higher than body temperature. Brain temperature started to fall at the outer border of the gray matter. The scalp temperature was ~36°C. Cold saline infusion resulted in a dose-dependent drop in ipsilateral white and gray matter temperature. The minimum temperature of 29.8°C was reached with a saline infusion rate of 50 ml/min. Inter- and intrahemispheric temperature gradients from the heat conduction between the warm contralateral and cooled ipsilateral hemisphere were significant. Similar temperature gradients were observed between the anterior and posterior circulation territories of the ipsilateral hemisphere (results not shown). Figure 3 also shows the radial temperature distribution along the same V-shaped *A-B* line in a brain with ischemic stroke. Cold saline infusion resulted in a dose-dependent drop in ipsilateral white and gray matter temperature. The temperature drop for a given saline infusion rate was larger than the corresponding temperature drop in the healthy brain. For example, an infusion rate of 50 ml/min resulted in a minimum temperature of 28.2°C at the ischemic core. Table 6 summarizes the mean ipsilateral anterior circulation territory brain

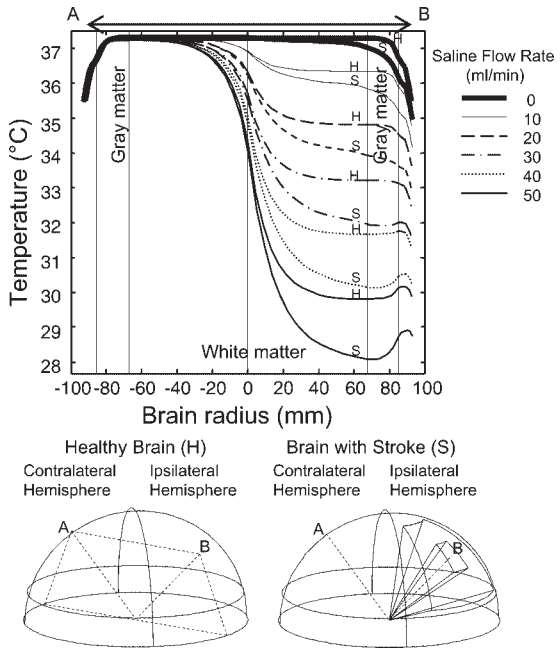

Fig. 3. Spatial temperature distribution 60 min after different rates of saline infusion in a healthy brain (H) and a brain with stroke (S). Temperature was sampled along *A-B* line (dashed). V-shaped *line A-B* begins at a latitude of 45°, descends to the center-base of the brain, and ascends back to the same latitude, in a longitudinal plane from −135° to +45°. Longitudinal plane dissects posterior circulation territory of the contralateral hemisphere to anterior territory of the ipsilateral hemisphere (dashed), via the center of the brain (see Fig. 1*C*). In the brain with stroke, *A-B* line passes through the stroke core.

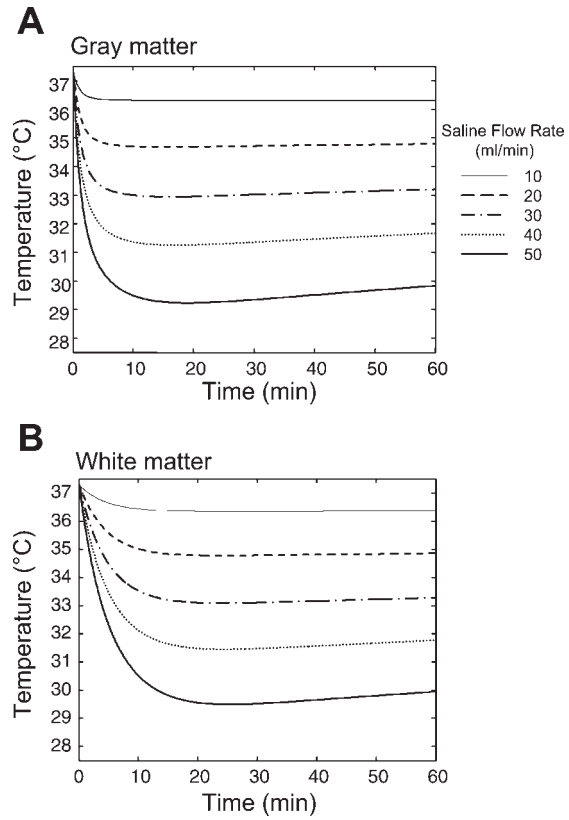

Fig. 4. Effect of different saline infusion rates on transient temperature profiles of gray (*A*) and white (*B*) matter in a healthy brain. Spatial location of temperature-sampling points is described in Fig. 1*C* (●).

temperatures after 60 min of cold saline infusion in a healthy brain and a brain with stroke.

The effect of different saline infusion rates on the transient temperature profiles of the gray and white matter of healthy brain is shown in Fig. 4. Faster infusion rates resulted in faster rates of hypothermia induction and lower brain temperatures. The gray matter cooled faster than the white matter for any given infusion rate. Mild-to-moderate hypothermia (<35°C) was reached within 10 min for saline infusion rates >20 ml/min.

The temperature drop in the gray and white matter of ischemic stroke core, penumbra, and noninfarcted tissue is summarized in Fig. 5. Here also, faster infusion rates resulted in faster rates of hypothermia induction and lower brain temperatures. Gray matter cooled faster than white matter for every tested infusion rate. The transient temperature profiles were distinctively different for the ischemic core, the penumbra, and the noninfarcted tissue for any given infusion rate. Hypothermia was induced almost twice as fast in the noninfarcted tissue as in the ischemic core. On the other hand, the ischemic core reached lower temperatures than tissue located in an identical location of healthy brain (Figs. 5, *A* and *B,* and 6). The transient temperature profile demonstrated that ischemic penumbra temperature was greater than core temperature but less than noninfarcted tissue temperature. Brain temperatures started to increase slowly but steadily after the minimum temperature was reached (Figs. 4 and 5).

Table 6. *Mean ipsilateral anterior circulation territory brain temperatures after 60 min of cold saline infusion*

Cold Saline Infusion Rate, ml/min	Mean Temp, °C				
	Healthy brain	Brain with ischemic stroke			
	IACT	IACT	Noninfarcted tissue	Ischemic penumbra	Ischemic core
10	36.39	36.07	36.22	35.83	35.80
20	35.03	34.37	34.59	33.99	34.00
30	33.60	32.64	32.94	32.11	32.14
40	32.22	31.03	31.41	30.36	30.41
50	30.57	29.23	29.72	28.39	28.46

IACT, ipsilateral anterior circulation territory.

The ipsilateral carotid blood flow in a healthy brain and in a brain with ischemic stroke under different saline infusion rates is shown in Fig. 6*A*. According to baseline white and gray matter perfusion values and *Eq. 12,* ICA blood flow rate before cold saline infusion in a healthy brain was ~250 ml/min, corresponding to published values (4, 45, 50, 51). Figure 6*A* shows that the initial blood flow rate was reset to >250 ml/min after induction of the saline infusion. The initial blood flow rate was lower in the brain with ischemic stroke (Fig. 6*A*), because blood perfusion is lower in ischemic brain tissue (54). In the case of stroke, saline infusion also reset the blood flow rate to higher values, although they still did not exceed 250 ml/min. Blood flow dropped rapidly in the stroke and nonstroke cases and started to increase soon after it reached the minimum rate. The minimum blood flow rate and minimum brain temperature were reached simultaneously (Figs. 4, 5, and 6*A*). The slow

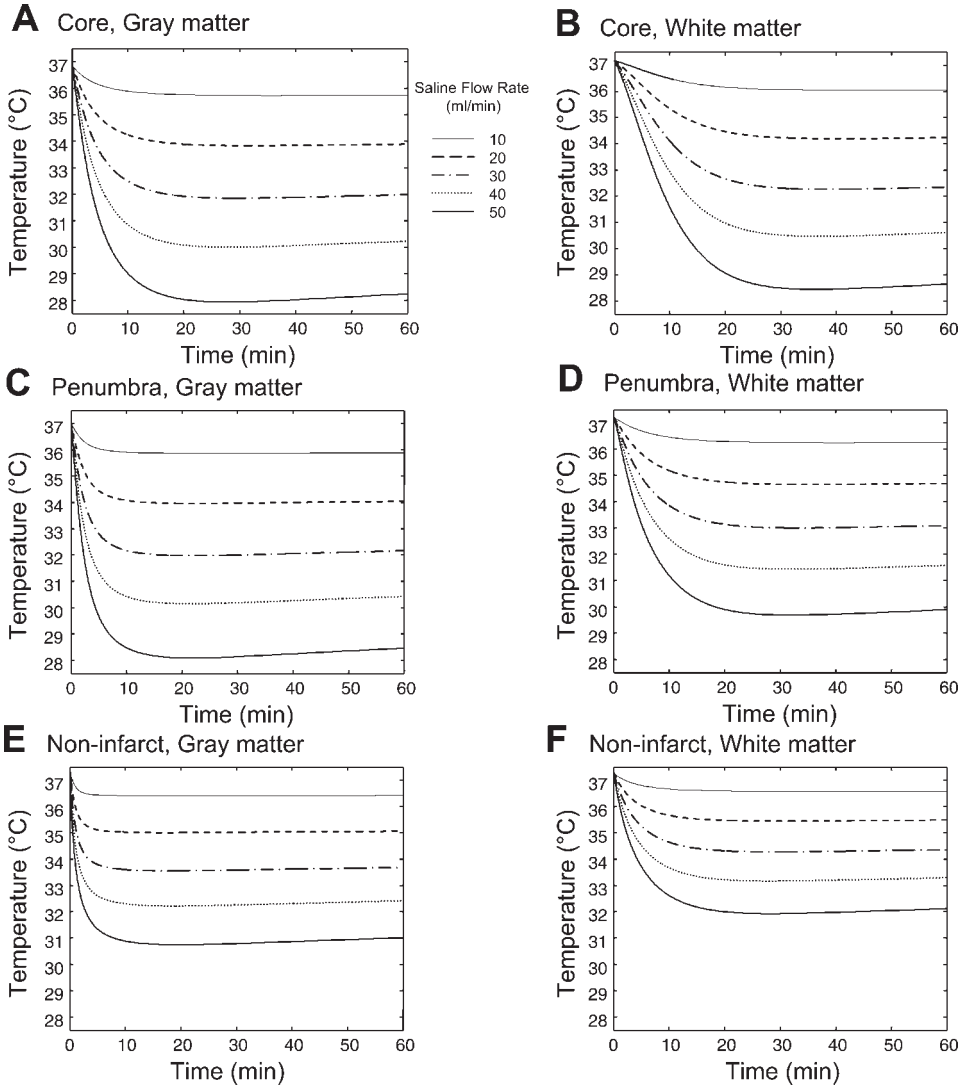

Fig. 5. Effect of different saline infusion rates on transient temperature profiles of gray (*A, C*, and *E*) and white (*B, D*, and *F*) matter of a brain with ischemic stroke. Spatial location of temperature-sampling points is described in Fig. 1*C* [●, ischemic core (*A* and *B*); ∗, ischemic penumbra (*C* and *D*); ▲, noninfarcted tissue (*E* and *F*)].

increase in ipsilateral carotid flow rate, which resulted from hemodilution, caused the slow secondary increase in brain temperature. Increasing blood flow rates resulted in a proportionally larger contribution of warm blood to the cold perfusate, thereby slowly increasing its temperature (Fig. 6*B*). The lower ipsilateral carotid flow rates and the resulting lower cold perfusate temperatures (Table 5) in the brain with ischemic stroke account for the lower brain temperatures achieved in the brain with stroke.

The decrease of hematocrit arising from saline infusion was estimated using data from human studies (Table 3). The effect of different rates of hypervolemic hemodilution on hematocrit, with the assumption of an initial hematocrit of 42%, is examined in Fig. 7. After 60 min of saline infusion at 50 ml/min, hematocrit was predicted to drop to 33.5%. Lower infusion rates resulted in smaller systemic hematocrit changes. Because of the saline infusion, the hematocrit of the perfusate reaching the brain supplied by ICA blood (local hematocrit) is lower than the systemic hematocrit at any given time. This happens because the saline infusion will result in an instantaneous drop of the perfusate hematocrit owing to the addition of the saline volume to the ipsilateral carotid blood. For the region of the brain supplied by the ICA, it is more appropriate to follow the decrease of local hematocrit with time. In this case, 60 min of saline infusion at 50 ml/min in a brain with stroke decreased the local hematocrit to a minimum of 25%. The continuous drop of local hematocrit became the force increasing the carotid blood flow rate once the minimum brain temperature had been reached after ~15 min. The gradual increase in warm core blood flow rate resulted in an increase in perfusate temperature that slowly increased the temperature of the cooled ipsilateral anterior circulation territory in the brain.

The decrease in whole body temperature caused by a 1.8°C saline infusion, applied at a flow rate of 50 ml/min over 60 min, is approximated using *Eq. 14* and is 1.82°C. This is the maximum theoretically possible systemic decrease in body temperature that is possible when the ipsilateral anterior circulation territory temperature has dropped to 30.57°C. In reality, the systemic cooling will probably be less than the maximum theoretical prediction. Cooling will primarily have a local effect, due to the nearly perfect local heat exchange in the brain vasculature (56), resulting in a minimal drop of core body temperature.

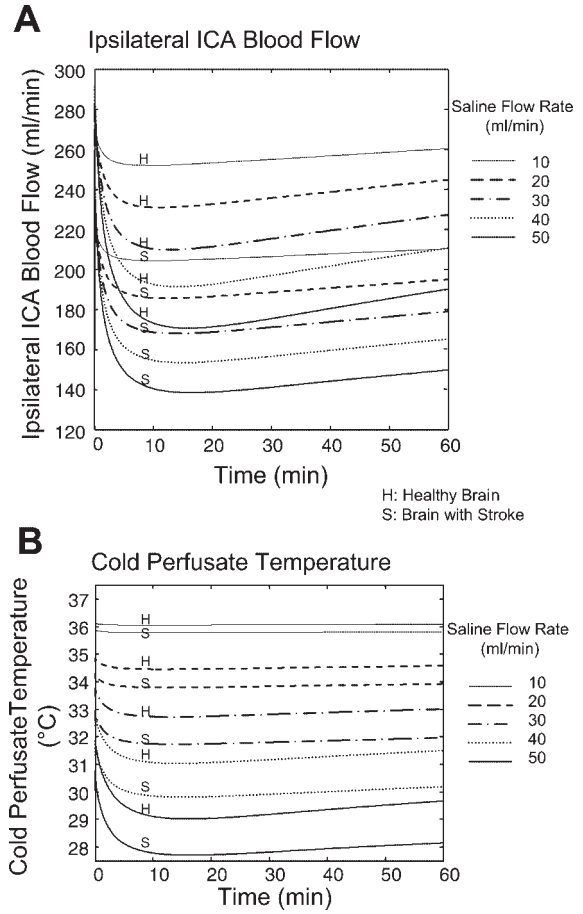

Fig. 6. *A*: effect of different saline infusion rates on ipsilateral internal carotid artery (ICA) blood flow rate in a healthy brain and a brain with ischemic stroke. *B*: effect of different saline infusion rates on cold perfusate temperature in a healthy brain and a brain with ischemic stroke.

DISCUSSION

Novel aspects of the present model. The present theoretical model examines the effect of a continuously changing blood perfusion rate (CBF) and perfusate temperature on brain temperature. Previous mathematical models investigated the effect of transcranial cooling in humans and assumed a constant CBF and perfusate temperature (44, 60) or a continuously changing CBF and a constant perfusate temperature (11, 68, 69). The models that employed a variable CBF as a function of temperature extrapolated the analytic expression for this relation directly from the expression for the metabolic heat generation as a function of brain temperature (*Eq. 1*) (11, 68, 69), whereas the present model fitted data from studies to quantify the expression more precisely.

To the best of our knowledge, only one other theoretical brain cooling model incorporated an ischemic region; however, it did not distinguish between ischemic penumbra and core (11). Using data for CBF and cerebral metabolic rate, the present model simulated the core and penumbra. In this study, blood perfusion data from patients assessed with PET and MRI were used to simulate the ischemic region of the brain (54).

Implications of the results. The model suggested that, during ICSI, temperature is the dominant regulatory parameter of CBF. Moderate ICSI rates (i.e., 30 ml/min) are sufficient to induce mild-to-moderate hypothermia (33–34°C) in the ipsilateral anterior circulation territory. Higher saline infusion rates can decrease the brain temperature below 30°C. These results are in sharp contrast to theoretical analyses (11, 44, 60) and intracerebral temperature monitoring studies in humans (8, 35), which demonstrate that transcranial cooling can reduce the temperature only in the superficial 1–2 cm of the brain. The proposed effectiveness of cold saline infusion and the corresponding ineffectiveness of cooling helmets to induce SBC support Baker's original statement that arterial temperature is the primary determinant of brain temperature (2). In the present model, brain temperature was always <1°C higher than the corresponding perfusate temperature.

It is estimated that hypothermia will be achieved within 10 min of the initiation of cold saline infusion. This is 18–42 times faster than the 3–7 h needed for whole body cooling by noninvasive methods (26, 52) and 10–20 times faster than whole body endovascular cooling (15). The present results suggest that ICSI is the only potential method of hypothermia induction with the ability to cool the ipsilateral brain fast enough so as not to miss the therapeutic window. Moreover, the fast induction of hypothermia may lengthen the therapeutic window and allow the combination with other interventions, such as intra-arterial tissue-type plasminogen activator and mechanical embolectomy.

ICSI is predicted to decrease systemic hematocrit and result in even larger reductions of local hematocrit. Saline infusion for 60 min at 30 and 50 ml/min decreased the local hematocrit

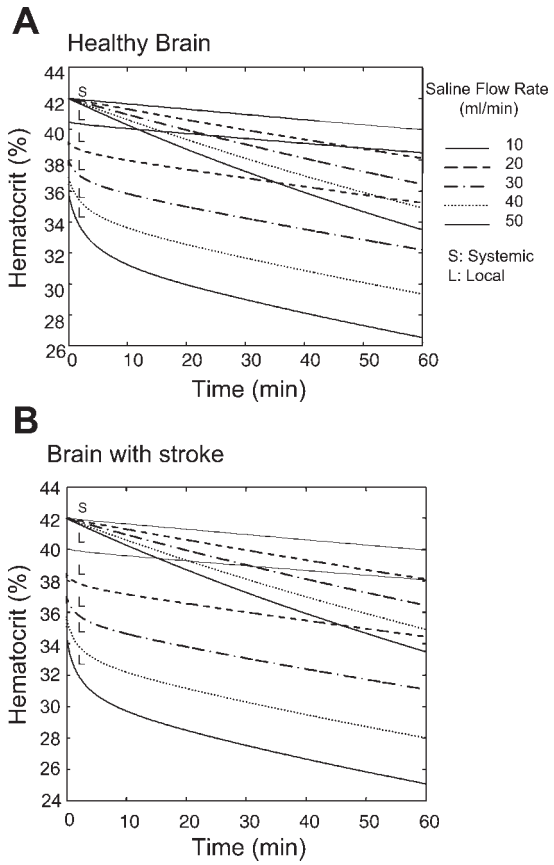

Fig. 7. Effect of different saline infusion rates on systemic and local (i.e., perfusate) hematocrit in a healthy brain (*A*) and a brain with stroke (*B*).

to 31% and 25%, respectively. Decades of experience with cardiopulmonary bypass operations have established hematocrit values in the very low 20s as the lowest acceptable levels in terms of safety (7). Thus, theoretically, hypothermia can be safely maintained for a maximum of 90 min at an infusion rate of 50 ml/min and 180 min at an infusion rate of 30 ml/min. Current evidence suggests that postischemic hypothermia in humans must be maintained for ≥12 h to be effective (21). It is clear that ICSI cannot be maintained for >3 h. Its potential role in the management of ischemic stroke is as the "igniter" for rapid induction of hypothermia in order not to miss the therapeutic window. At the same time, systemic hypothermia can be applied via endovascular cooling for the maintenance of hypothermia after a couple of hours.

The present model makes a number of predictions about the temperature distributions in the brain. *1*) The model predicts a steady-state preinfusion deep brain temperature that is 0.3°C higher than the body core temperature. This is the same deep brain-body core temperature gradient reported by Rossi et al. (49) in 20 neurological patients. *2*) There is a small temperature gradient between the cerebral surface and deeper parenchyma under steady-state conditions. This gradient is consistent with data comparing superficial with ventricular or deep parenchymal temperatures in normothermic patients (36, 58). *3*) The model predicts significant inter- and intrahemispheric temperature gradients resulting from the heat conduction between brain tissues receiving warm blood supply and tissues receiving the cold perfusate. Similar temperature gradients have been reported in pigs (30) and dogs (64) undergoing SBC via anterograde cerebral perfusion of extracorporeally cooled blood. The agreement between the model predictions and the published human and animal data provide evidence of the model's fidelity to an in vivo scenario.

Limitations of the model. The present model has several limitations. *1*) The geometry of the head was modeled as a hemisphere, but the real shape of the head is not exactly hemispherical. However, careful selection of an appropriate dimension yielded a brain volume of 1,285 ml, which is intermediate between the volume of the average male and the volume of the average female brain (29). *2*) The model used human thermal, physical, and physiological data for the four different tissues it incorporated (white matter, gray matter, skull, and scalp) but omitted the dura matter and the cerebrospinal fluid. This layer was omitted because it is too thin (~2 mm) (44), and the thermal properties of the cerebrospinal fluid are very similar to those of the brain tissue (11, 44). *3*) Pennes' equation describes a continuum model where heat and mass transport are averaged over a representative unit volume. Continuum models are not able to predict the variation in temperature in the immediate vicinity of large, discrete blood vessels. However, the results obtained from a discrete vessel thermal model agreed well with Pennes' continuum model (60). *4*) The present model assumes that the cerebrovascular response to hypothermia and hemodilution is near instantaneous. There are no data for the temporal characteristics of the cerebrovascular responses to hypothermia and hemodilution. However, initiation of local tissue hypoxia with sensory stimulation of cortical columns resulted in vascular responses within 1–3 s (32), indicating that the cerebrovascular response is fast. *5*) Systemic cooling was not taken into account, and the core body temperature was clamped at 37°C. Hence, the carotid blood mixing with the cold infusate had a temperature of 37°C at all times. In reality, carotid blood temperature will drop slightly as the core body temperature falls due to cool jugular venous return. *6*) Heat transfer between brain tissues of the anterior and posterior circulation territories and between the two hemispheres was modeled only by conduction. Convective heat transfer between the anterior and posterior circulation territories via the posterior communicating artery and between the hemispheres via the anterior communicating artery was not considered. The extensive pial collaterals of the anterior and posterior cerebral arteries were also excluded (10). Moreover, modification of the flow dynamics between different brain regions by the stroke is possible (10). The present model, however, does not take into account any blood transfer between these different brain regions normally perfused by the carotid or basilar arteries. *7*) The model assumes that temperature and hematocrit control the CBF independently. In theory, it is plausible, although not likely, that a reduced hematocrit may modify the cerebrovascular response to hypothermia, and vice versa.

In conclusion, this model is an attempt to determine the feasibility of SBC with ICSI. The results suggest that SBC can be achieved rapidly using moderate saline flow rates. Moreover, infarcted brain tissue can reach even lower temperatures than noninfarcted tissue for a given saline infusion rate. These results are encouraging and call for a more extensive evaluation of invasive SBC in animal models of focal ischemia. If the extensive experience with endovascular procedures and the short therapeutic window after ischemic stroke are taken into account, invasive SBC is a realistic management option for ischemic stroke patients.

ACKNOWLEDGMENTS

The authors thank Hui Zhang for technical assistance and Dr. Jae H Choi, Christine Dumoulin, and Yi-Ting Chiang for constructive comments.

The research was performed in partial fulfillment of the requirements for the Ph.D. degree by M. A. Neimark in the Department of Biomedical Engineering, Columbia University.

GRANTS

This study was supported by NYSTAR.

REFERENCES

1. **Almeida MF.** Preoperative normovolemic hemodilution in aesthetic plastic surgery. *Aesthetic Plast Surg* 23: 445–449, 1999.
2. **Baker MA.** Brain cooling in endotherms in heat and exercise. *Annu Rev Physiol* 44: 85–96, 1982.
3. **Bauer R, Fritz H, Walter B, Schlonski O, Jochum T, Hoyer D, Zwiener U, Reinhart K.** Effect of mild hypothermia on cerebral oxygen uptake during gradual cerebral perfusion pressure decrease in piglets. *Crit Care Med* 28: 1128–1135, 2000.
4. **Boyajian RA, Schwend RB, Wolfe MM, Bickerton RE, Otis SM.** Measurement of anterior and posterior circulation flow contributions to cerebral blood flow. An ultrasound-derived volumetric flow analysis. *J Neuroimaging* 5: 1–3, 1995.
5. **Bruder N, Cohen B, Pellissier D, Francois G.** The effect of hemodilution on cerebral blood flow velocity in anesthetized patients. *Anesth Analg* 86: 320–324, 1998.
6. **Chen H, Chopp M, Zhang ZG, Garcia JH.** The effect of hypothermia on transient middle cerebral artery occlusion in the rat. *J Cereb Blood Flow Metab* 12: 621–628, 1992.
7. **Cook DJ, Oliver WC Jr, Orszulak TA, Daly RC, Bryce RD.** Cardiopulmonary bypass temperature, hematocrit, and cerebral oxygen delivery in humans. *Ann Thorac Surg* 60: 1671–1677, 1995.
8. **Corbett RJ, Laptook AR.** Failure of localized head cooling to reduce brain temperature in adult humans. *Neuroreport* 9: 2721–2725, 1998.

9. **De Dear RJ, Arens E, Hui Z, Oguro M.** Convective and radiative heat transfer coefficients for individual human body segments. *Int J Biometeorol* 40: 141–156, 1997.
10. **Derdeyn CP, Powers WJ, Grubb RL Jr.** Hemodynamic effects of middle cerebral artery stenosis and occlusion. *Am J Neuroradiol* 19: 1463–1469, 1998.
11. **Diao C, Zhu L, Wang H.** Cooling and rewarming for brain ischemia or injury: theoretical analysis. *Ann Biomed Eng* 31: 346–353, 2003.
12. **Ehrlich MP, McCullough JN, Zhang N, Weisz DJ, Juvonen T, Bodian CA, Griepp RB.** Effect of hypothermia on cerebral blood flow and metabolism in the pig. *Ann Thorac Surg* 73: 191–197, 2002.
13. **Ekelund A, Reinstrup P, Ryding E, Andersson AM, Molund T, Kristiansson KA, Romner B, Brandt L, Saveland H.** Effects of iso- and hypervolemic hemodilution on regional cerebral blood flow and oxygen delivery for patients with vasospasm after aneurysmal subarachnoid hemorrhage. *Acta Neurochir (Wien)* 144: 703–712, 2002.
14. **Feigin V, Anderson N, Gunn A, Rodgers A, Anderson C.** The emerging role of therapeutic hypothermia in acute stroke. *Lancet* 2: 529, 2003.
15. **Georgiadis D, Schwarz S, Kollmar R, Schwab S.** Endovascular cooling for moderate hypothermia in patients with acute stroke: first results of a novel approach. *Stroke* 32: 2550–2553, 2001.
16. **Grathwohl KW, Bruns BJ, LeBrun CJ, Ohno AK, Dillard TA, Cushner HM.** Does hemodilution exist? Effects of saline infusion on hematologic parameters in euvolemic subjects. *South Med J* 89: 51–55, 1996.
17. **Greenfield RH, Bessen HA, Henneman PL.** Effect of crystalloid infusion on hematocrit and intravascular volume in healthy, nonbleeding subjects. *Ann Emerg Med* 18: 51–55, 1989.
18. **Harris BA, Andrews PJD.** Direct brain cooling. In: *Therapeutic Hypothermia*, edited by Mayer SA and Sessler DI. New York: Dekker, 2005, p. 323–386.
19. **Henriksen L, Paulson OB, Smith RJ.** Cerebral blood flow following normovolemic hemodilution in patients with high hematocrit. *Ann Neurol* 9: 454–457, 1981.
20. **Hino A, Ueda S, Mizukawa N, Imahori Y, Tenjin H.** Effect of hemodilution on cerebral hemodynamics and oxygen metabolism. *Stroke* 23: 423–426, 1992.
21. **Holzer M, Bernard SA, Hachimi-Idrissi S, Roine RO, Sterz F, Mullner M; on behalf of the Collaborative Group on Induced Hypothermia for Neuroprotection After Cardiac Arrest.** Hypothermia for neuroprotection after cardiac arrest: systematic review and individual patient data meta-analysis. *Crit Care Med* 33: 414–418, 2005.
22. **Iguchi A, Haneda K, Sato S, Horiuchi T.** Determination of safe interval of circulatory arrest from the cerebral metabolic aspect. *Tohoku J Exp Med* 149: 191–204, 1986.
23. **Jalan R, Damink SW, Deutz NE, Lee A, Hayes PC.** Moderate hypothermia for uncontrolled intracranial hypertension in acute liver failure. *Lancet* 354: 1164–1168, 1999.
24. **Jalan R, Olde Damink SW, Deutz NE, Davies NA, Garden OJ, Madhavan KK, Hayes PC, Lee A.** Moderate hypothermia prevents cerebral hyperemia and increase in intracranial pressure in patients undergoing liver transplantation for acute liver failure. *Transplantation* 75: 2034–2039, 2003.
25. **Johansen LB, Bie P, Warberg J, Christensen NJ, Hammerum M, Videbaek R, Norsk P.** Hemodilution, central blood volume, and renal responses after an isotonic saline infusion in humans. *Am J Physiol Regul Integr Comp Physiol* 272: R549–R556, 1997.
26. **Kammersgaard LP, Rasmussen BH, Jorgensen HS, Reith J, Weber U, Olsen TS.** Feasibility and safety of inducing modest hypothermia in awake patients with acute stroke through surface cooling: a case-control study: the Copenhagen Stroke Study. *Stroke* 31: 2251–2256, 2000.
27. **Kass LE, Tien IY, Ushkow BS, Snyder HS.** Prospective crossover study of the effect of phlebotomy and intravenous crystalloid on hematocrit. *Acad Emerg Med* 4: 198–201, 1997.
28. **Kawamura S, Suzuki A, Hadeishi H, Yasui N, Hatazawa J.** Cerebral blood flow and oxygen metabolism during mild hypothermia in patients with subarachnoid haemorrhage. *Acta Neurochir (Wien)* 142: 1117–1121, 2000.
29. **Koh I, Lee MS, Lee NJ, Park KW, Kim KH, Kim H, Rhyu IJ.** Body size effect on brain volume in Korean youth. *Neuroreport* 16: 2029–2032, 2005.
30. **Kuhnen G, Bauer R, Walter B.** Controlled brain hypothermia by extracorporeal carotid blood cooling at normothermic trunk temperatures in pigs. *J Neurosci Methods* 89: 167–174, 1999.
31. **Labiche LA, Grotta JC.** Clinical trials for cytoprotection in stroke. *NeuroRx* 1: 46–70, 2004.
32. **Malonek D, Grinvald A.** Interactions between electrical activity and cortical microcirculation revealed by imaging spectroscopy: implications for functional brain mapping. *Science* 272: 551–554, 1996.
33. **Marion DW, Obrist WD, Carlier PM, Penrod LE, Darby JM.** The use of moderate therapeutic hypothermia for patients with severe head injuries: a preliminary report. *J Neurosurg* 79: 354–362, 1993.
34. **Maruyama M, Shimoji K, Ichikawa T, Hashiba M, Naito E.** The effects of extreme hemodilutions on the autoregulation of cerebral blood flow, electroencephalogram and cerebral metabolic rate of oxygen in the dog. *Stroke* 16: 675–679, 1985.
35. **Mellergard P.** Changes in human intracerebral temperature in response to different methods of brain cooling. *Neurosurgery* 31: 671–677, 1992.
36. **Mellergard P, Nordstrom CH.** Epidural temperature and possible intracerebral temperature gradients in man. *Br J Neurosurg* 4: 31–38, 1990.
37. **Merrill TL.** Thermodynamics and heat transfer. In: *Therapeutic Hypothermia*, edited by Mayer SA and Sessler DI. New York: Dekker, 2005, p. 265–292.
38. **Metz C, Holzschuh M, Bein T, Woertgen C, Frey A, Frey I, Taeger K, Brawanski A.** Moderate hypothermia in patients with severe head injury: cerebral and extracerebral effects. *J Neurosurg* 85: 533–541, 1996.
39. **Michenfelder JD, Milde JH.** The relationship among canine brain temperature, metabolism, and function during hypothermia. *Anesthesiology* 75: 130–136, 1991.
40. **Michenfelder JD, Milde JH, Katusic ZS.** Postischemic canine cerebral blood flow is coupled to cerebral metabolic rate. *J Cereb Blood Flow Metab* 11: 611–616, 1991.
41. **Mori K, Maeda M, Miyazaki M, Iwase H.** Effects of mild (33°C) and moderate (29°C) hypothermia on cerebral blood flow and metabolism, lactate, and extracellular glutamate in experimental head injury. *Neurol Res* 20: 719–726, 1998.
42. **Muhling J, Dehne MG, Sablotzki A, Hempelmann G.** Cerebral blood flow velocity during isovolemic hemodilution and subsequent autologous blood retransfusion. *Can J Anaesth* 46: 550–557, 1999.
43. **Nagel K, Ghussen F, Kruger I, Isselhard W.** Miniature equipment for the perfusion of rat limbs. *Res Exp Med (Berl)* 187: 1–8, 1987.
44. **Nelson DA, Nunneley SA.** Brain temperature and limits on transcranial cooling in humans: quantitative modeling results. *Eur J Appl Physiol* 78: 353–359, 1998.
45. **Oktar SO, Yucel C, Karaosmanoglu D, Akkan K, Ozdemir H, Tokgoz N, Tali T.** Blood-flow volume quantification in internal carotid and vertebral arteries: comparison of 3 different ultrasound techniques with phase-contrast MR imaging. *Am J Neuroradiol* 27: 363–369, 2006.
46. **Origitano TC, Wascher TM, Reichman OH, Anderson DE.** Sustained increased cerebral blood flow with prophylactic hypertensive hypervolemic hemodilution ("triple-H" therapy) after subarachnoid hemorrhage. *Neurosurgery* 27: 729–740, 1990.
47. **Pennes HH.** Analysis of tissue and arterial blood temperature in the resting human forearm. *J Appl Physiol* 1: 93–122, 1948.
48. **Rosomoff HL, Holaday DA.** Cerebral blood flow and cerebral oxygen consumption during hypothermia. *Am J Physiol* 179: 85–88, 1954.
49. **Rossi S, Zanier ER, Mauri I, Columbo A, Stocchetti N.** Brain temperature, body core temperature, and intracranial pressure in acute cerebral damage. *J Neurol Neurosurg Psychiatry* 71: 448–454, 2001.
50. **Scheel P, Ruge C, Petruch UR, Schoning M.** Color duplex measurement of cerebral blood flow volume in healthy adults. *Stroke* 31: 147–150, 2000.
51. **Schoning M, Walter J, Scheel P.** Estimation of cerebral blood flow through color duplex sonography of the carotid and vertebral arteries in healthy adults. *Stroke* 25: 17–22, 1994.
52. **Schwab S, Georgiadis D, Berrouschot J, Schellinger PD, Graffagnino C, Mayer SA.** Feasibility and safety of moderate hypothermia after massive hemispheric infarction. *Stroke* 32: 2033–2035, 2001.
53. **Schwartz AE, Stone JG, Finck AD, Sandhu AA, Mongero LB, Adams DC, Jonassen AE, Young WL, Michler RE.** Isolated cerebral hypothermia by single carotid artery perfusion of extracorporeally cooled blood in baboons. *Neurosurgery* 39: 577–581, 1996.
54. **Shimosegawa E, Hatazawa J, Ibaraki M, Toyoshima H, Suzuki A.** Metabolic penumbra of acute brain infarction: a correlation with infarct growth. *Ann Neurol* 57: 495–504, 2005.
55. **Shiozaki T, Sugimoto H, Taneda M, Yoshida H, Iwai A, Yoshioka T, Sugimoto T.** Effect of mild hypothermia on uncontrollable intracranial hypertension after severe head injury. *J Neurosurg* 79: 363–368, 1993.

56. **Slotboom J, Kiefer C, Brekenfeld C, Ozdoba C, Remonda L, Nedeltchev K, Arnold M, Mattle H, Schroth G.** Locally induced hypothermia for treatment of acute ischaemic stroke: a physical feasibility study. *Neuroradiology* 46: 923–934, 2004.
57. **Stamler KD.** Effect of crystalloid infusion on hematocrit in nonbleeding patients, with applications to clinical traumatology. *Ann Emerg Med* 18: 747–749, 1989.
58. **Stone JG, Goodman RR, Baker KZ, Baker CJ, Solomon RA.** Direct intraoperative measurement of human brain temperature. *Neurosurgery* 41: 20–24, 1997.
59. **Tu YK, Liu HM.** Effects of isovolemic hemodilution on hemodynamics, cerebral perfusion, and cerebral vascular reactivity. *Stroke* 27: 441–445, 1996.
60. **Van Leeuwen GM, Hand JW, Lagendijk JJ, Azzopardi DV, Edwards AD.** Numerical modeling of temperature distributions within the neonatal head. *Pediatr Res* 48: 351–356, 2000.
61. **Vorstrup S, Andersen A, Juhler M, Brun B, Boysen G.** Hemodilution increases cerebral blood flow in acute ischemic stroke. *Stroke* 20: 884–889, 1989.
62. **Walter B, Bauer R, Kuhnen G, Fritz H, Zwiener U.** Coupling of cerebral blood flow and oxygen metabolism in infant pigs during selective brain hypothermia. *J Cereb Blood Flow Metab* 20: 1215–1224, 2000.
63. **Weimar C, Mieck T, Buchthal J, Ehrenfeld CE, Schmid E, Diener HC; German Stroke Study Collaboration.** Neurologic worsening during the acute phase of ischemic stroke. *Arch Neurol* 62: 393–397, 2005.
64. **White RJ, Locke GE, Albin MS.** Isolated profound cerebral cooling with a bi-carotid heat exchanger shunt in dogs. *Resuscitation* 10: 193–195, 1983.
65. **Wood JH, Polyzoidis KS, Kee DB Jr, Prats AR, Gibby GL, Tindall GT.** Augmentation of cerebral blood flow induced by hemodilution in stroke patients after superficial temporal-middle cerebral arterial bypass operation. *Neurosurgery* 15: 535–539, 1984.
66. **Wysocki M, Andersson OK, Persson B, Bagge U.** Vasoconstriction during acute hypervolemic hemodilution in hypertensive patients is not prevented by calcium blockade. *Angiology* 49: 41–48, 1998.
67. **Wysocki M, Persson B, Aurell M, Braide M, Bagge U, Andersson OK.** Haemodynamic and haemorheological effects of hypervolaemic haemodilution in men with primary hypertension. *J Hypertens* 5: 185–189, 1987.
68. **Xu X, Tikuisis P, Giesbrecht G.** A mathematical model for human brain cooling during cold-water near-drowning. *J Appl Physiol* 86: 265–272, 1999.
69. **Zhu L, Diao C.** Theoretical simulation of temperature distribution in the brain during mild hypothermia treatment for brain injury. *Med Biol Eng Comput* 39: 681–687, 2001.